Gene Expression Pattern in Human Brain Endothelial Cells in Response to *Neisseria meningitidis*[▽][†]

Alexandra Schubert-Unkmeir,[1]* Olga Sokolova,[1,2] Ursula Panzner,[1]
Martin Eigenthaler,[2] and Matthias Frosch[1]

*Institute of Hygiene and Microbiology[1] and Institute of Clinical Biochemistry and
Pathobiochemistry,[2] University of Wuerzburg, Wuerzburg, Germany*

To extend our knowledge of target proteins in endothelial cells infected with the meningitis-causing pathogen *Neisseria meningitidis*, we characterized the interaction between the bacterial and human brain microvascular endothelial cell (HBMEC) monolayers. By use of human cDNA microarrays, transcriptional analysis revealed distinct responses to 4 and 8 h of infection. We also addressed the question of whether the major virulence factor of meningococci, i.e., the capsule, influences the host cell response. Of the 1,493 (at 4 h postinfection) and 1,246 (at 8 h postinfection) genes with altered expression upon bacterial contact, about 49.4% and 45%, respectively, depended on capsule expression. In particular, we identified an increase of expression for genes encoding proteins involved in bacterial adhesion and invasion. High levels of apoptosis-related gene (*bad, bak, asp,* and immediate-early response gene 1) expression could also be detected in infected cells. Further analyses confirmed that HBMECs displayed several hallmarks of apoptosis in response to *N. meningitidis* infection, namely, phosphatidylserine translocation and activation of caspase 3 and AMP-activated protein kinase α. Moreover, several differentially regulated genes not previously known to respond to meningococcal infection were identified. Of these, genes encoding cell adhesion proteins (CD44, CD98, and CD99), genes involved in downstream signaling of integrins (integrin-linked kinase, mitogen-activated protein kinase kinase 1, and mitogen-activated protein kinase kinase kinase 10) as well as negative regulators of these pathways (dual-specificity phosphatases 1, 5, and 14 and G protein pathway suppressor 2), and genes involved in cytoskeleton reorganization (those encoding Arp2/3, p34-arc, actinin alpha 1, vasodilatator-stimulated protein, and Wiskott-Aldrich syndrome protein) were the most prominent. This global transcriptional analysis creates a new platform for further molecular and cellular analysis of the interaction between *N. meningitidis* and target cells.

The gram-negative bacterium *Neisseria meningitidis* (meningococcus) remains a significant cause of morbidity and mortality in developed and developing nations. The meningococcus is a common colonizing bacterium of the human nasopharynx that in a small percentage of carriers crosses the epithelial barrier and gets access to the bloodstream. Following bacteremia, *N. meningitidis* may bind and subsequently cross the blood-cerebrospinal fluid (B-CSF) barrier to enter the subarachnoideal space, resulting in acute and purulent meningitis (43). To overcome the barrier, the bacterium has evolved the ability to invade and pass through the host cell. Three meningococcal cell components are clearly essential for meningeal invasion: (i) the capsular polysaccharide, which is required for bacterial survival in extracellular fluids, (ii) type IV pili, multimeric structures essential for the adhesion of virulent capsulated *N. meningitidis* to host cells (41, 42, 61), and (iii) the Opc outer membrane protein, facilitating entry into brain endothelial cells (60, 62).

The group B polysaccharide capsule, the most dominant capsular type in Europe, is composed of a homopolymeric α(2→8) *N*-acetyl neuraminic acid (polysialic acid) (2). This capsule is an important virulence determinant which protects the meningococcus against complement-mediated bacteriolysis and phagocytosis (17, 62). Mutants deficient in capsule expression are serum sensitive and nonpathogenic.

Recent studies based on DNA array technology examined the repertoire of cellular responses towards infection with pathogenic *Neisseria*. Wells et al. used cDNA arrays to identify a cytoprotective response to *N. meningitidis* in meningothelial cells (64). The same group also profiled gene expression in meningothelial cells in response to secreted meningococcal proteins (51). Binnicker and coworkers found up-regulation of several host antiapoptotic factors in urethral epithelial cells infected with *Neisseria gonorrhoeae*, a close relative of meningococci (3). Bonnah et al. discovered the alteration of several host genes involved in iron homeostasis (5). Finally, Plant and coworkers used cDNA microarrays to compare epithelial cell responses towards piliated and nonpiliated *N. gonorrhoeae* cells and pilated encapsulated meningococci (47).

While these studies demonstrated the induction of genes encoding proinflammatory cytokines, apoptosis-related proteins, and cell surface molecules by *N. meningitidis*, the existing literature provides little information about bacterium-mediated effects on the host cell function, cytoskeleton organization, monolayer integrity, and cell receptor abundance or secreted molecules other than cytokines. However, endothelial

organization plays an important role in pathogenesis of meningococcal disease, since endothelial damage and capillary leakage were shown to be the basis of tissue injury in septicemia (11, 25, 27, 36). Furthermore, the endothelial cell cytoskeleton has been shown to participate in cell invasion by *N. meningitidis* (24). As cellular receptors and surface markers exposed on the host cells during meningococcal infection could be interesting markers and targets for the diagnosis and treatment of meningococcal meningitis, we sought to study the translocation of the B-CSF barrier by meningococci, extending existing studies (1, 21, 45, 48, 53, 56, 60). For this purpose, we took advantage of the availability of high-density microarrays, which we applied to characterize the expression of about 11,835 different human genes in human brain microvascular endothelial cells (HBMEC) in response to infection with meningococci. The results of this study indicate that meningococci regulate transcription of a wide range of genes involved in transcription, translation, and cell metabolism and genes encoding intracellular transducers. In addition, we identified several differentially regulated genes not previously known to respond to *N. meningitidis* infection.

MATERIALS AND METHODS

Bacterial strains. *Neisseria meningitidis* strain MC58 (B15:P1.7,16b) and the MC58 *siaD* unencapsulated mutant (60) were routinely cultured in proteose-peptone medium supplemented with 1% polyvitex (bioMérieux, Lyon, France) to the mid-logarithmic phase and diluted to approximately 1×10^7 CFU in RPMI 1640 medium (Biochrom AG, Berlin, Germany) supplemented with 10% heat-inactivated (30 min at 56°C) human serum for all cell culture experiments.

Endothelial cell culture. HBMEC were isolated from a brain biopsy of an adult female with epilepsy, transfected with the simian virus 40 large T antigen, and cultured as described previously (55, 56). HBMEC maintained their morphological and functional characteristics of primary brain endothelial cells for up to 15 passages. Cells were cultured in RPMI 1640 medium, supplemented with fetal calf serum (10%), Nu serum IV (10%), vitamins (1%), nonessential amino acids (1%), sodium pyruvate (1 mM), L-glutamine (2 mM), heparin (5 U ml^{-1}) (all reagents were from Biochrom, Berlin, Germany), and endothelial cell growth supplement (30 μg ml^{-1}) (Habor Costar Corporation, Cambridge, MA). The cells were maintained in T25 flasks (Corning Costar Corporation, Cambridge, MA) coated with 0.2% gelatin in a humid atmosphere at 37°C with 5% CO$_2$. For microarray experiments and real-time PCR (LightCycler; Roche), the cells were used at passage 10. For further experiments, passages 10 to 15 were used.

HBMEC infection. For microarray hybridization and real-time PCR experiments, HBMEC were split and seeded onto T75 flasks at a density of 0.5×10^7 cells per flask and cultured for 48 h. Two hours prior to infection, confluent cell monolayers were washed three times with RPMI 1640 medium. HBMEC were infected with either wild-type (WT) strain M58 or the MC58 *siaD* capsule mutant strain at a multiplicity of infection (MOI) of 10. Control cells received fresh RPMI 1640 supplemented with 10% heat-inactivated human serum. After 4 hours and 8 hours of infection, bacteria were removed and HBMEC were washed three times with phosphate-buffered saline (PBS; Biochrom AG, Berlin, Germany), trypsinized as described before (12), resuspended in ice-cold PBS, and centrifuged at 1,000 × *g* for 5 min at 4°C. The snap-frozen pellets were then stored at −70°C for RNA isolation.

For fluorescence-activated cell sorter (FACS) analysis and enzyme-linked immunosorbent assay (ELISA) experiments, HBMEC were seeded onto 12-well plates (Corning Costar Corporation, Cambridge, MA) at a density of 1×10^5 per well 2 days prior to the experiments. The cells were washed and infected as described above. After 8, 16, and 24 h of infection, supernatants were collected for cytokine assessment, centrifuged at 10,000 × *g* for 5 min at 4°C, and frozen for storage at −70°C. For FACS analysis, cell monolayers were washed twice with RPMI 1640 medium. Cells were detached with 0.25% trypsin and washed once with PBS following specific FACS protocol.

RNA isolation, cDNA preparation, and hybridization. Total RNA was extracted with saturated phenol-chloroform and precipitated in isopropanol, and pellets were washed with 80% ethanol, dried, and resuspended in RNase-free H$_2$O. Subsequently, total RNA was treated with DNase in the presence of

1 U ml^{-1} anti-RNase (Ambion) and 45 μg of total RNA was used for poly(A)$^+$ RNA enrichment using a BD Atlas Pure Total RNA labeling system kit (BD Bioscience Clontech, Palo Alto, CA) and [^{33}P]-dADP (Amersham Pharmacia, Hong Kong). Labeled cDNA was separated from unincorporated nucleotides with NucleoSpin extraction spin columns following hybridization onto prerinsed plastic microarrays at 60°C for 14 h according to the manufacturer's instructions (BD Atlas plastic human 12K microarray kit; BD Bioscience Clontech, Palo Alto, CA). The microarrays were washed twice with 2× SSC-0.1% sodium dodecyl sulfate (SDS) (1× SSC is 0.15 M NaCl plus 0.015 M sodium citrate) and twice with 0.1× SSC-0.1% SDS for 5 min at 60°C in all cases and then twice with 0.1× SSC at 30°C for 5 min each time.

Array analysis. For the cDNA microarray experiments, BD Atlas plastic human 12K microarrays (BD Bioscience Clontech) were used. The array contains a selection of 11,835 human genes (oligonucleotides), including 9 housekeeping genes, cDNA synthesis controls, and negative controls (various phage λ sequences) printed in duplicate on a plastic support surface. Equal amounts of labeled probes from MC58- and MC58 *siaD* strain-infected and uninfected cells were hybridized to the microarrays according to the manufacturer's instructions. After the washing procedure (twice with 2× SSC-0.1% SDS and twice with 0.1× SSC-0.1% SDS for 5 min at 60°C in all cases and then twice with 0.1× SSC at 30°C for 5 min each time) was completed, the arrays were exposed with a low-energy phosphorimaging screen (Molecular Dynamics, CA) overnight and for 3 days. The signal intensities were detected with Imager Analyzer FLA-3000 using "Image Reader" soft (Fuji Photo Film Co., Ltd.) at 50-μm resolution. The intensities of cDNA double spots from infected and uninfected cells were compared, and the data were exported as Excel files for further analysis. The probes were stripped from the arrays following the manufacturer's recommendations and then rehybridized with newly labeled probes. The resulting expression profiles were virtually identical to those from the first hybridization, but with only 70% of the original intensities. This phenomenon has already been described by other users of this cDNA microarray platform (30). We also presented data only from the first experiment, in agreement with published data.

Arrays were further analyzed using AtlasImage 2.7 software (Clontech) according to the manufacturer's guidelines. Using AtlasImage 2.7 software, the arrays were aligned with a BD AtlasImage grid template (BD Clontech) automatically and then fine-tuned for each gene by using manual adjustment options. The background was calculated based on the median intensity of the "blank spaces" between different panels of the array (default method of calculation), and the raw signal intensity of each spot was measured. A raw intensity (before normalization) of twofold over background was taken as an indication that a gene was expressed at a significant level. Using this criterion, we found 1,628 genes expressed in HBMEC at 4 h and 1,489 genes expressed at 8 h after infection with encapsulated meningococci (strain MC58) (Table 1). A list of all of the expressed genes is presented in the supplemental material. For comparison of the expression patterns of MC58-infected cells and uninfected cells, the signal intensities were normalized by the global normalization sum method, which is best suited for the comparison of two similar tissue samples. Signal values for arrays hybridized with MC58-infected cDNA were normalized with respect to those for arrays reprobed with cDNA of uninfected cells. The adjusted signal intensities of each of the individual cDNA spots were compared for infected and uninfected cells. The ratios (numerical values in Tables 2, 3, and 4) were calculated as the adjusted intensity of array 2 (infected HBMEC) divided by the adjusted intensity of array 1 (uninfected cells) according to the manufacturer's guidelines. Differences are estimated when a gene signal either in array 1 or in array 2 is at background level. Instead of using numerical values, we indicated these genes as up-regulated (↑) or down-regulated (↓) in infected HBMEC. The results were saved in a tab-delimited format and opened by Microsoft Excel for further analysis. To further search for significant changes of gene classes, we used GoMiner, a program that classifies genes into biological categories and calculates the probability of over- and underrepresentation within a particular group, compared with the master list by use of Fisher's exact test (65).

Real-time PCR. Differential gene expression data were validated using an SYBR green-based real-time quantitative PCR method. HBMEC were infected with the MC58 wild-type strain and the MC58 *siaD* mutant strain or exposed to RPMI medium supplemented with 10% heat-inactivated human serum, and at 4 h and 8 h postinfection (h p.i.), cell monolayers were washed and total RNA was extracted using an RNeasy mini kit (QIAGEN). The total RNA content was determined spectrophotometrically, and equal amounts of RNA were treated with RNase-free DNase (Roche). Total RNA (2 μg) was reverse transcribed with random nonamers (2.5 μM) using Omniscript reverse transcriptase (4 U ml^{-1}) according to the manufacturer's instructions.

For quantitative PCR, SYBR green master mix (Roche) was used according to the manufacturer's instructions.

TABLE 1. Gene expression profiles of HBMEC infected with strain MC58 at 4 h and 8 h postinfection[a]

Gene product functional classification	No. of genes with indicated MC58-infected HBMEC/uninfected HBMEC ratio at:					
	4 h p.i.			8 h p.i.		
	0.5 or less	0.5–<2.0	2.0 or more	0.5 or less	0.5–<2.0	2.0 or more
All	888	366	374	252	496	741
Cell surface antigens	11	3	4	1	7	11
Transcription	53	20	27	12	29	63
Cell cycle	5	6	6	4	7	6
Cell adhesion receptors/proteins	13	2	5	1	7	9
Immune system proteins	1	1	7		3	9
Extracellular transporter/carrier proteins	10	2	3	3	4	10
Oncogenes/tumor suppressors	9	6	2	2	7	10
Stress response proteins	7	4	3	3	8	5
Membrane channels and transporters	21	9	18	1	11	33
Extracellular matrix proteins	3		1	1		5
Trafficking/targeting proteins	24	14	10	8	21	28
Metabolism	56	63	63	17	70	82
Posttranslational/protein folding	25	16	12	7	19	21
Translation	13	46	40	23	45	34
Apoptosis-associated proteins	9	5	4	4	4	17
RNA processing/turnover/transport	21	12	9	6	15	21
DNA binding and chromatin proteins	10	5	10	4	5	12
Cell receptors	27	2	7	3		18
Cell signaling, extracellular communication proteins	23	5	5	3	7	24
Intracellular transducers/effectors/modulators	80	20	45	9	41	77
Protein turnover	20	15	14	6	17	28
Cell receptors (by activities)	6	3	2	1	1	9
Cytoskeleton/motility proteins	22	22	8	5	20	27
DNA synthesis/recombination/repair	11	4	5	3	4	13
Functionally unclassified	72	27	31	16	50	65
Not classified	336	54	32	109	94	104

[a] Genes with expression levels at least twofold over background.

Primers specific to immediate-early response gene 1 (forward, 5′-GAA CTG CGG CAA AGT AGG AG-3′; reverse, 5′-GAC AGT CGC TCC GTG ACA GC-3′), *bak* (forward, 5′-CGA CAT CAA CCG ACG CTA TG-3′; reverse, 5′-GCA ATG CAG TGA TGC AGC ATG-3′), *bad* (forward, 5′-TGG ATG ACC TCG ATG ATG AAG-3′; reverse, 5′-GCA CAG CAA CGC AGA TGC G-3′), *asp* (forward, 5′-CTG ACT CAC ATA CAG TAG ATC-3′; reverse, 5′-GGA TAC TAT GAT TTG ACA GGC-3′), and *req* (forward, 5′-CGT GGC TTC ACA CGC ACC-3′; reverse, 5′-AAG TGG GAG TGG GCA TAG TG-3′) were designed and used for amplification of 261-, 244-, 266-, 222-, and 208-bp amplicons, respectively.

Preliminary experiments showed that the β-actin transcription level was not affected under the experimental conditions to which the cells were subjected. The results were analyzed according to the method described by Pfaffl (46). For this mathematical method, the efficiency (E) of each PCR is calculated from the slopes of cDNA input versus the crossing points (CP) plot as follows: $E = 10^{(-1/slope)}$. The relative expression ratio of the gene of interest to the target gene was calculated with respect to the reference gene (β-actin gene) by comparing HBMEC infected with meningococci and untreated control cells. The ratio was calculated as follows: $(E_{target})^{\Delta CP\ target\ (control-sample)}/(E_{reference})^{\Delta CP\ reference\ (control-sample)}$.

Flow cytometry. Antibodies to intercellular adhesion molecule 1 (ICAM-1) (fluorescein isothiocyanate conjugated; Biosource, Camarillo, CA) were purchased and used in flow cytometric analysis to examine the protein expression in HBMEC. Briefly, following infection cells were blocked with 3% bovine serum albumin for 30 min, and cells were stained with anti-ICAM-1 (1:20) for 45 min at 4°C. Following staining, cells were fixed with 1% paraformaldehyde for 15 min and analyzed by fluorescence measurement. Mouse immunoglobulin G1 fluorescein isothiocyanate conjugate (Biosource, Camarillo, CA) was used as described above and served as an isotype control. For apoptosis detection, an annexin V-biotin kit (Immunotech, France) was used. Following infection, cells were collected, washed, and stained with 5% annexin V-biotin solution in 1× binding buffer (PBS containing 5.5 mM D-glucose and 0.5% bovine serum albumin) for 10 min. Subsequently, cells were fixed with 1% paraformaldehyde (methanol free; Polysciences, Warrington, PA) for bacterial killing. Cells were washed once with annexin V-biotin solution in 1× binding buffer and incubated with 20 mg ml⁻¹ streptavidin-phycoerythrin conjugate for 20 min. All staining steps were conducted on ice. Flow cytometric analyses were performed on a FACSCalibur flow cytometer (Becton Dickinson) and analyzed using CellQuest software, version 3.1.

Cell lysate preparation and Western blotting. At various time points of infection, cells were washed three times with PBS. Washed cells were lysed in 1× SDS sample buffer directly on a plate, collected, and boiled for 5 min. Cellular proteins were resolved by 10% (Akt and AMP-activated protein kinase α [AMPK-α]) or 15% (caspase 3) SDS-polyacrylamide gel electrophoresis and electrotransferred to nitrocellulose membranes (Schleicher & Schuell, Dassel, Germany). After being blocked for 1 h in Tris-buffered saline–Tween (25 mM Tris, pH 7.6, 150 mM NaCl, 0.05% Tween 20) containing 6% dry milk (Bio-Rad, Munich, Germany), membranes were incubated with primary antibodies at 4°C overnight. The following antibodies were used: rabbit anticleaved caspase 3 (Asp175), anti-phospho-AMPK-α (Thr1729), and anti-phospho-Akt (Ser437) (Cell Signaling Technology Inc., Beverly, MA). Membranes were washed briefly and incubated with horseradish peroxidase-conjugated anti-rabbit immunoglobulin G (Bio-Rad, Munich, Germany) secondary antibodies (1:3,000 in 3% dry milk–Tris-buffered saline–Tween 20) for 50 min at room temperature. Immunoreactivity was detected using an ECL or ECL Plus detection kit (Amersham Pharmacia Biotech, Freiburg, Germany). To detect endogenous levels of activated proteins, blots were stripped and reprobed with antibodies specific to the nonphosphorylated form of the protein of interest. The protein bands on X-ray films were scanned by using a StudioStar imaging densitometer, Agfa, and the intensities of bands were analyzed using NIH Image software.

Cytokine assessment by ELISA of HBMEC supernatants. Concentrations of interleukin-6 (IL-6) and tumor necrosis factor alpha (TNF-α) in the cell culture supernatants were measured by commercially available ELISA kits (AMS Biotechnology GmbH, Abington, United Kingdom). The ELISAs were performed according to the manufacturer's instructions to a sensitivity of 4 pg ml⁻¹. For all ELISA systems, the 3,3′,5,5′-tetramethyl(benzidine) (TMB) substrate reagent set (BD Pharmingen, Heidelberg, Germany) was used to detect the streptavidin-horseradish peroxidase (BD Pharmingen) reaction. All samples were assayed in duplicate. The experiments were carried out at least four times.

RESULTS

Expression profile of HBMEC induced by *N. meningitidis*. To investigate the effect of meningococcal infection on the transcriptome of HBMEC, we used BD Atlas plastic human 12K microarrays (BD Clontech). This cDNA-based microarray platform contains 11,835 different human genes. HBMEC were used already as a valuable tool for studying the translocation of the B-CSF barrier by meningitis-causing pathogens (1, 21, 45, 48, 60). To discriminate changes of the transcriptome, both infected and control cells were analyzed 4 h and 8 h after infection with meningococci. At 4 h p.i., bacteria reached saturation of adhesion to HBMEC with only low invasion, whereas at 8 h p.i., a maximum of bacteria was internalized (60).

These analyses revealed that 366 genes showed similar levels of expression in MC58-infected and uninfected HBMEC at 4 h p.i. (Table 1). A total of 374 genes (30% of genes with a ratio of at least twofold) were up-regulated in MC58-infected cells, and 888 genes (70%) were down-regulated. After a period of 8 h of infection, the activity of gene expression turned around: while 741 genes (74.6%) were overexpressed in MC58-infected cells, 252 genes (25.4%) were down-regulated (Table 1). A total of 496 genes showed similar levels of expression in infected and uninfected HBMEC.

The expressed genes comprise all functional categories (Table 1): transcription (100 genes at 4 h p.i. and 104 genes at 8 h p.i.; $P < 0.01$ as analyzed with GoMiner), membrane channel proteins and transporters (48 at 4 h p.i. and 45 at 8 h p.i.; $P < 0.01$), metabolism (182 at 4 h p.i. and 169 at 8 h p.i.; $P < 0.01$), posttranslational modification/protein folding (53 at 4 h p.i. and 47 at 8 h p.i.; $P = 0.57$), protein translation (99 at 4 h p.i. and 102 at 8 h p.i.; $P = 0.05$), intracellular transducers/effectors/modulators (145 at 4 h p.i. and 127 at 8 h p.i.; $P = 0.42$), and cytoskeleton/motility proteins (52 at 4 h p.i. and 52 at 8 h p.i.; $P = 0.0024$) were detected. A total of 552 genes (4 h p.i.) and 438 genes (8 h p.i.) that have not been functionally classified or are unclassified were also expressed at elevated levels. Further analysis revealed that at 4 h p.i., most of the genes were of low abundance (70%) and about 30% of them were expressed at levels at least 10-fold over background. At the late stage of infection, only 42% of the genes were of low abundance and 58% of them were at levels at least 10-fold over background.

Table 2 categorizes the most notable genes and their 4-h and 8-h induction values. The highest levels of induction were observed for genes encoding ribosomal proteins with levels at least 10-fold over background, such as ribosomal proteins L10a, L27, and S15a (Table 2).

Cell surface antigens. Five cell adhesion molecules were expressed at relative high levels in MC58-infected cells. Among them, the hyaluronate receptors CD44, CD98, and CD99 were the most prominent. CD44 mediates human cell-cell- and cell-extracellular matrix-binding interactions and has also been described to function as a receptor for group A streptococcus colonization of the pharynx in vivo (10). Inter-

nalization of piliated capsulated meningococci has been shown to be triggered by the formation of microvillus-like membrane protrusion, containing eszin, moesin, and the integral membrane proteins CD44 and ICAM-1 (24). Atlas plastic human 12K microarrays also contained cDNAs for ICAM-1 (CD54), and mRNA for ICAM-1 was also shown to be highly expressed with 5-fold and 18-fold expression levels over background at 4 h p.i. and 8 h p.i., respectively (Table 2), while expression in uninfected HBMEC was undetectable. To verify whether the changes in ICAM-1 mRNA levels were reflected by protein expression, flow cytometry of immunostained MC58-infected and uninfected HBMEC was performed. After 8 h of incubation, a marked increase of ICAM-1-positive events (34%) was detected (Fig. 1A and B), and 16 h after infection, 62% of events from cultures were ICAM-1 positive compared to those from uninfected cells.

Interestingly, a substantial level of CD98 was expressed in MC58-infected HBMEC at 4 h p.i. and 8 h p.i. CD98 acts as an important regulator of integrin-mediated adhesion (50). It is constitutively associated with β_1 integrins regardless of the activation status. We previously described that invasion of *N. meningitidis* in HBMEC is mediated by $\alpha_5\beta_1$ integrins (60). In accordance with data from Plant and colleagues (47), the gene encoding the integrin β_1 chain was not up-regulated. However, levels of the integrin α_5 transcript were significantly increased (Table 2).

Intracellular transducers/effectors/modulators. Infected cells expressed genes involved in downstream signaling of $\alpha_5\beta_1$ integrins and of other receptors such as ICAM-1 and CD44, including integrin-linked kinase (ILK), Rho GTPase-activating protein 1, and regulatory enzymes such as guanine nucleotide exchange factors (e.g., Rho Gef12) (Table 2). Two further members of the RAS superfamily (*rhoG* and *rhoC*) were highly up-regulated at 4 h p.i. and 8 h p.i. in MC58-infected cells. We furthermore observed regulated genes involved in the mitogen-activated protein kinase (MAPK) signaling pathway: MAP kinase kinase 1 and MAP kinase kinase kinase 10 were down-regulated after infection. While MAP kinase kinase 1 regulates the extracellular signal-regulated kinase signaling pathway, MAP kinase kinase kinase 10 has been shown to function preferentially on the Jun N-terminal protein kinase signaling pathway (52). At 8 h of infection, dual-specificity phosphatases (DUSPs) 1, 5, and 14 and G protein pathway suppressor 2 (GPS2) were found to be up-regulated in infected cells, indicating expression of genes involved in negative regulation of downstream MAPK signaling pathways.

Cell signaling/extracellular communication proteins. Another finding of the comparative gene expression analysis was that low, but clearly above background, levels of multiple cytokines and chemokines were observed in MC58-infected cells (Table 2). The genes of the cytokines IL-6, TNF-α, chemokine-like factor 1, CC chemokine CCL19 (macrophage inflammatory protein 3β and EBI1 ligand chemokine), and insulin-like growth factor 1 (somatomedin C) were up-regulated in infected cells. IL-1α, insulin-like growth factor 2 (somatomedin A), inducible VGF nerve growth factor, and CC chemokine member 22 (SCYA22) were down-regulated at the analyzed time points.

IL-6 and TNF-α have already been shown to be induced by *N. meningitidis* upon infection of meningothelial and endothe-

TABLE 2. HBMEC transcription profile after infection with strain MC58 at 4 h p.i. and 8 h p.i.

Category and array location	MC58-infected HBMEC/uninfected HBMEC ratio at[a]:		Gene or protein description/name	GenBank accession no.
	4 h p.i.	8 h p.i.		
Cell surface antigens				
O18ab4	0.333	0.262	CD63 antigen (melanoma 1 antigen)	NM_001780
I14ab6	↓	*	Integrin beta 2 (CD18 antigen [p95])	NM_000211
H14cd1	↓	*	Selectin P ligand	NM_003006
K15ef5	↓	*	CD4 antigen (p55)	M12807
E13ab2	*	↑	Acrosomal vesicle protein 1	NM_001612
G23ab7	↑	↑	Antigen identified by monoclonal antibodies 12E7, F21, and O13 (CD99)	NM_002414
E21ab7	↑	3.047	Solute carrier family 3, member 2 (CD98)	NM_002394
O21ef1	3.4	2.85	CD44 antigen	M59040
P07ab3	0.263	3.049	CD3E antigen, epsilon polypeptide (TiT3 complex)	NM_000733
Transcription				
J21cd7	0.176	0.409	Paired box gene 9	NM_006194
H08ef1	0.333	0.161	SCAN domain-containing 1	NM_016558
J06ef6	0.375	0.294	Nucleobindin 1	M96824
M17ef5	0.166	*	Heat shock transcription factor 1	M64673
B07ef1	0.143	*	Nuclear factor I/C (CCAAT-binding transcription factor)	X12492
N17ef6	0.107	0.722	CCAAT/enhancer binding protein alpha	U34070
B17ab8	0.479	0.929	Polymerase (RNA) II (DNA-directed) polypeptide G	NM_002696
P07cd7	↑	↑	General transcription factor IIIC, polypeptide 5 (63 kDa)	NM_012087
N21cd2	↑	↑	Requiem, apoptosis response zinc finger gene	NM_006268
F02ef6	↑	*	Immediate-early protein	M62831
P23ef6	↑	↑	B-cell CLL/lymphoma 3	M31732
B01cd7	3.72	3.677	Kruppel-like factor 8	NM_007250
D24ef6	4.0	*	Early growth response 1	M62829
G01cd3	57.0	5.12	Ribosomal protein S27 (metallopanstimulin 1)	NM_001030
P03cd3	0.583	2.1	Inhibitor of kappa light polypeptide gene enhancer in B cells, kinase gamma	NM_003639
Cell cycle				
B13ef5	0.2	0.6	Mitogen-activated protein kinase 3	X60188
B21ef5	↓	*	Mitogen-activated protein kinase 7	U25278
H01ef5	↑	1.909	CDC37 cell division cycle 37 homolog (*Saccharomyces cerevisiae*)	U63131
H23ef5	↑	0.217	CDC20 cell division cycle 20 homolog (*S. cerevisiae*)	U05340
K12ab5		*	Cyclin F	NM_001761
O08ef5	*	↑	Cyclin D3	M92287
O04ef5	*	↑	Cyclin D1 (parathyroid adenomatosis 1)	X59798
C01ab4	0.714	↑	Cyclin-dependent kinase 8	NM_001260
D03ef5	*	↑	Cyclin-dependent kinase 9 (CDC2-related kinase)	L25676
B23ef5	*	↑	Cyclin-dependent kinase (CDC2-like) 10	L33264
Cell adhesion receptors				
F04cd7	↓	*	Claudin 12	NM_012129
F06cd7	↓	*	Claudin 14	NM_012130
E17ef4	↓	0.555	Protocadherin 17	NM_014459
G14ab8	0.0869	0.737	Protocadherin 8	NM_002590
G21ef7	0.607	0.490	Laminin receptor 1 (67 kDa, ribosomal protein SA)	U43901
F23ab3	0.111	↑	Glycoprotein Ib (platelet) beta polypeptide	NM_000407
B17ab3	↓	*	Glycoprotein IX (platelet)	NM_000174
I02ab6	↑	↑	Intercellular adhesion molecule 1 (CD54), human rhinovirus receptor	NM_000201
E23ef7	*	↑	Integrin alpha 5 (fibronectin receptor, alpha polypeptide)	X06256
Immune system proteins				
B16ef7	↑	↑	TAP binding protein (tapasin)	AF009510
A01cd2	2.833	2.646	Major histocompatibility complex class IC	M11886
C23ab3	2.0	↑	Beta-2-microglobulin	NM_004048
E15ef1	2.50	↑	Immunoglobulin heavy constant epsilon	J00222
Oncogenes and tumor suppressors				
A08ef5	0.25	↑	Platelet-derived growth factor beta polypeptide (simian sarcoma viral [v-*sis*] oncogene homolog)	X02811
A20cd4	1.471	5.933	FOS-like antigen 1	NM_005438
D21ab5	*	↑	FOS-like antigen 2	NM_005253
M14ab7	↓	*	v-*myc* myelocytomatosis viral oncogene homolog 2 (avian)	NM_005377
G02ef5	*	0.290	v-*myb* myeloblastosis viral oncogene homolog (avian)-like 2	X13293
Stress response proteins				
E20ef7	0.3	0.207	Heme oxygenase (decycling) 1	X06985
G20ef7	0.462	0.633	Superoxide dismutase 1	K00065
K14ab7	↓	*	Heat shock 70-kDa protein 1B	NM_005346
K13ef5	↓	*	Heat shock 70-kDa protein 1A	M11717
D19cd8	*	↑	Hypoxia-inducible protein 2	NM_013332

TABLE 2—*Continued*

Category and array location	MC58-infected HBMEC/uninfected HBMEC ratio at[a]:		Gene or protein description/name	GenBank accession no.
	4 h p.i.	8 h p.i.		
Membrane channels and transporters				
O10ab2	0.143	↑	Aquaporin 6, kidney specific	NM_001652
O14ab2	0.154	*	Aquaporin 8	NM_001169
O16ab8	4.174	5.584	Proteolipid protein 2 (colonic epithelium enriched)	NM_002668
P18ab2	2.5	↑	ATP synthase, H$^+$ transporting, mitochondrial F1 complex, O subunit	NM_001697
A21ab2	3.5	↑	ATP-binding cassette, subfamily A, member 4	NM_000350
L22ab2	↑	↑	ATPase, Na$^+$/K$^+$ transporting, beta 1 polypeptide	NM_001677
A15ab2	↑	*	ATP-binding cassette, subfamily A, member 1	NM_005502
A21ab2	*	↑	ATP-binding cassette, subfamily A, member 4	NM_000350
Extracellular matrix proteins				
O24cd6	↑	↑	Cartilage-associated protein	NM_006371
O05ab5	↓	*	Extracellular matrix protein 1	NM_004425
D05ab7	↓	↑	Ladinin 1	NM_005558
Trafficking/targeting proteins				
F15ab5	0.656	0.424	Clathrin, light polypeptide (Lca)	NM_001833
H02ef1	*	↑	Protein kinase C/casein kinase substrate in neuron 3	NM_016223
P24ab3	*	↑	Caveolin 3	NM_001234
Metabolism				
A01cd8	1.665	1.076	Glyceraldehyde-3-phosphate dehydrogenase	X01677
N15cd1	0.739	0.611	Transketolase (Wernicke-Korsakoff syndrome)	NM_001064
A04cd1	2.0	3.6	Phytanoyl-coenzyme A hydroxylase (Refsum disease)	NM_006214
A07ab3	0.166	↓	ATPase, H$^+$ transporting, lysosomal 42-kDa V1 subunit C, isoform 1	NM_001695
A12ab8	1.8	5.412	Ornithine decarboxylase 1	NM_002539
B07ab3	↑	↑	Galactosidase alpha	NM_000169
C04cd2	5.5	2.058	Thymidine kinase 1, soluble	NM_003258
A20ab6	1.652	1.082	Cytochrome *c* oxidase subunit VIb	NM_001863
E17ab6	0.25	0.545	Cytochrome *c* oxidase subunit VIa polypeptide 2	NM_005205
G02ab5	4.416	1.964	Cytochrome *c* oxidase subunit VIIa polypeptide 2 (liver)	NM_001865
J08ab4	0.333	2.545	Enolase 2 (gamma, neuronal)	NM_001975
J16ab8	0.333	0.312	NADH dehydrogenase (ubiquinone) Fe-S protein 3 (30 kDa) (NADH-coenzyme Q reductase)	NM_004551
J18ab8	1.666	0.5	NADH dehydrogenase (ubiquinone) Fe-S protein 5 (15 kDa) (NADH-coenzyme Q reductase)	NM_004552
J20ab8	1.428	0.5	NADH dehydrogenase (ubiquinone) Fe-S protein 6 (13 kDa) (NADH-coenzyme Q reductase)	NM_004553
P16ab8	5.0	3.3	NADH dehydrogenase (ubiquinone) 1 beta subcomplex 9 (22 kDa, B22)	NM_005005
L01ab7	20.0	1.039	Malate dehydrogenase 2, NAD (mitochondrial)	NM_005918
Posttranslational modification/protein folding				
A21cd8	0.375	*	Hsp70-interacting protein	NM_012267
K10ef1	↓	*	Heat shock 70-kDa protein 2	U56725
H24ef2	↑	↑	Heat shock protein 75	NM_016292
J06ef2	↓	*	DnaJ (Hsp40) homolog, subfamily B, member 11	NM_016306
B02ab7	*	↑	DnaJ (Hsp40) homolog, subfamily B, member 2	NM_006736
P21ab2	↑	↑	ADP-ribosylation factor 4	NM_001660
Translation				
F21cd1	1.3	0.209	Ribosomal protein, large, P0	NM_001002
P12ef1	0.673	0.374	Ribosomal protein L13a	X56932
H15cd1	0.738	0.277	Ribosomal protein S11	NM_001015
G22cd1	6.687	5.333	Ribosomal protein L10a	NM_007104
F01cd1	25.0	5.821	Ribosomal protein L27	NM_000988
H23cd1	25.5	1.714	Ribosomal protein S15a	NM_001019
Apoptosis-associated proteins				
A08ef6	0.1	0.466	Adenosine A1 receptor	S56143
L11cd2	0.166	↑	TNF receptor-associated factor 1	NM_005658
E20ef6	0.333	*	v-*akt* murine thymoma viral oncogene homolog 1	M63167
G14ef6	0.344	0.363	Defender against cell death 1	D15057
I15ef5	0.455	1.615	Tumor necrosis factor (ligand) superfamily, member 7	L08096
G04ef6	3.0	↑	Immediate-early response 3	AF071596
L10ef3	↓	*	Tumor necrosis factor receptor superfamily, member 21	NM_014452
G18ef6	↓	*	Death-associated protein 3	X83544

TABLE 2—*Continued*

Category and array location	MC58-infected HBMEC/uninfected HBMEC ratio at[a]:		Gene or protein description/name	GenBank accession no.
	4 h p.i.	8 h p.i.		
K24ef1	↑	↑	Bcl2 antagonist of cell death	U66879
N04ab3	*	↑	Bcl2 antagonist/killer 1	NM_001188
N23ab2	↑	↑	APG5 autophagy 5 like (*S. cerevisiae*)	NM_004849
C03cd7	*	↑	FAST kinase[b]	NM_006712
Cell receptors (by ligands)				
G13ef5	0.143	0.142857	Gamma interferon receptor	A09781
N01cd1	0.25	0.25	Somatostatin receptor 3	NM_001051
A09ab7	↓	*	Lymphotoxin beta receptor (TNF receptor superfamily, member 3)	NM_002342
P01ab3	↑	↑	Cholecystokinin A receptor	NM_000730
G07ab2	*	↑	Activin A receptor type I	NM_001105
G11ab2	*	↑	Activin A receptor type II	NM_001616
G09ab2	*	↑	Activin A receptor type IB	NM_004302
Cell signaling/extracellular communication proteins				
D09ab6	↓	*	Insulin-like growth factor 2 (somatomedin A)	NM_000612
F15ef7	↓	*	Interleukin 1 alpha	X02851
C20cd3	↓	*	VGF nerve growth factor inducible	NM_003378
O24ef7	*	↑	Insulin-like growth factor 1 (somatomedin C)	M27544
F21ef7	*	↑	Interleukin 6 (interferon beta 2)	X04602
I10ef7	*	↑	Tumor necrosis factor alpha-induced protein 2	M92357
N05ef4	*	2.2	Chemokine-like factor 1	NM_016326
P05cd2	*	↑	Small inducible cytokine subfamily, member 19	NM_006274
F10cd1	↓	*	Small inducible cytokine subfamily, member 22	NM_002990
Intracellular transducers/ effectors/modulators				
K09ab7	0.111	*	Mitogen-activated protein kinase kinase kinase 10	NM_002446
G15cd5	0.113	0.75	Dual-specificity tyrosine phosphorylation-regulated kinase 1B	NM_004714
N10ab8	0.166	0.862	Mitogen-activated protein kinase kinase kinase 2	NM_004579
B14ab2	0.182	↑	Arg/Abl-interacting protein ArgBP2	NM_003603
E12cd3	0.2	↓	Wiskott-Aldrich syndrome-interacting protein	NM_003387
P16cd5	0.207	1.727	RAS guanyl-releasing protein 2 (calcium and diacylglycerol regulated)	NM_005825
J12ef5	0.25	*	Mitogen-activated protein kinase kinase 3	L36719
F02ef5	0.666	4.9	EphA2	M59371
H08ef5	2.0	1.692	Integrin-linked kinase	U40282
B20ab2	2.5	↑	Ras homolog gene family, member G (Rho G)	NM_001665
B16ab2	3.222	6.31	Ras homolog gene family, member C	NM_005167
C03ef6	7.0	1.443	ADP-ribosylation factor 1	M36340
H23ef7	↓	*	EphA5	U26403
J08ef5	↓	↑	Mitogen-activated protein kinase kinase 1	L05624
L14ef5	↓	*	Janus kinase 3	U09607
M22ab5	↑	↑	Dual-specificity phosphatase 1	NM_004417
D04ab2	↑	*	Ras homolog gene family, member H	NM_004310
B22ab2	↑	↑	Rho GTPase-activating protein 1	NM_004308
P03ef3	↑	*	Rho guanine nucleotide exchange factor 12	NM_015313
A16ab5	*	↑	G protein pathway suppressor 2	NM_004489
K01ef6	*	↑	Interferon regulatory factor 1	X14454
M22ab5	*	↑	Dual-specificity phosphatase 1	NM_004417
B21ab4	*	↑	Dual-specificity phosphatase 5	NM_004419
O15cd7	*	↑	Dual-specificity phosphatase 14	NM_007026
Protein turnover				
H23ab8	↑	*	Protease, serine 7 (enterokinase)	NM_002772
N23ef7	↑	*	Cathepsin D (lysosomal aspartyl protease)	M11233
E01ab5	↑	2.545	Cathepsin B	NM_001908
P19ef7	*	↑	Plasminogen activator, urokinase	M15476
Cytoskeleton/motility proteins				
E18cd6	0.25	0.515	Myosin, light polypeptide 9, regulatory	NM_006097
L06cd6	0.13	1.6	WASP family, member 3	NM_006646
F04ab2	1.166	2.0	Actin-related protein 2/3 complex, subunit 1A (41 kDa)	NM_006409
C08cd3	0.5	*	Vasodilator-stimulated phosphoprotein	NM_003370
B04cd2	*	↑	Talin 1	NM_006289
E23ab2	0.512	2.218	Actinin alpha 1	NM_001102
A06ab6	1.577	2.444	Actin gamma 1	NM_001614
C24cd3	2.3	2.833	Vimentin	NM_003380
A08ab6	0.3	↑	Actin gamma 2, smooth muscle, enteric	NM_001615
D19ab2	*	↑	Actin-related protein 3 homolog (yeast)	NM_005721

TABLE 2—Continued

Category and array location	MC58-infected HBMEC/uninfected HBMEC ratio at[a]:		Gene or protein description/name	GenBank accession no.
	4 h p.i.	8 h p.i.		
F08ab2	1.666	↑	Actin-related protein 2/3 complex, subunit 2 (34 kDa)	NM_005731
E17ab2	↓	↑	Actin alpha 2, smooth muscle, aorta	NM_001613
Not classified				
C05gh3	3.333	*	Hypoxia-inducible factor 1-responsive RTP801	NM_019058

[a] The ratios (numerical values) were calculated as the adjusted intensity of array 2 (MC58-infected HBMEC) divided by the adjusted intensity of array 1 (uninfected HBMEC) according to the manufacturer's guidelines. Differences are estimated when a gene signal either in array 1 or in array 2 is at background level. Instead of numerical values, genes are indicated as up-regulated (↑) or down-regulated (↓) in MC58-infected HBMEC. * indicates genes with signal intensities of at least twofold over background in MC58-infected and uninfected cells.

[b] FAST kinase, Fas-activated serine/threonine kinase.

lial cells (51, 53, 64). To analyze whether changes in mRNA levels were reflected in protein expression, ELISAs were performed for the detection of IL-6 and TNF-α protein secretion. Supernatants from infected and uninfected HBMEC cultured for 16 h were analyzed, and the concentrations of both cytokines, IL-6 and TNF-α, were markedly elevated in the supernatants obtained at 8 h of infection ($P < 0.05$) and peaked at 16 h p.i. (Fig. 2). At 16 h p.i., the concentration of IL-6 was 5.3 times higher in response to MC58-infected cells than in response to control cells. TNF-α was not detectable in uninfected cells, but its concentration increased in supernatants from infected cells up to 96.3 ± 9.3 pg ml^{-1} at 16 h p.i. However, genes for many other proinflammatory markers produced by epithelial or endothelial cells in response to bacterial pathogens (e.g., IL-8 and growth-related oncogenes α and β, which belong to the CXC subfamily of chemokines) were not induced in HBMEC by *N. meningitidis* at 4 h p.i. and 8 h p.i.

Cell adhesion receptors/proteins. The array data represent cDNAs for a number of cell adhesion proteins that have been reported to play an important role in maintaining cellular integrity. The mRNAs that showed a decrease in MC58-infected cells were claudin 12, claudin 14, protocadherin 8, and protocadherin 17. Claudins are transmembrane proteins of tight junctions and take part in the regulation of brain endothelial permeability (35). Protocadherins constitute the largest subgroup within the cadherin family of calcium-dependent cell-cell adhesion molecules and are assumed to be anchored to the cytoskeleton (18).

Cytoskeleton/motility proteins. Our analysis also showed a strong enrichment of factors that interact with the host cell cytoskeleton ($P = 0.0024$). Several genes involved in the reorganization of the cytoskeleton or genes encoding motility proteins, e.g., the actin-related protein 3 (ARP3) homolog, the actin-related protein 2/3 complex, subunit 2 (p34-Arc), the mRNA of actinin alpha 1 (ACTN1), and cytoskeletal gamma actin as well as alpha 2 actin, were up-regulated in MC58-infected cells mainly at the late the stage of infection, indicating cytoskeleton rearrangements in the context of bacterial internalization. Although a number of genes involved in cell cytoskeleton and motility were up-regulated as mentioned above, two components of the host cell cytoskeleton machinery were found to be down-regulated: the vasodilatator-stimulated protein (VASP), which is involved in the regulation of actin
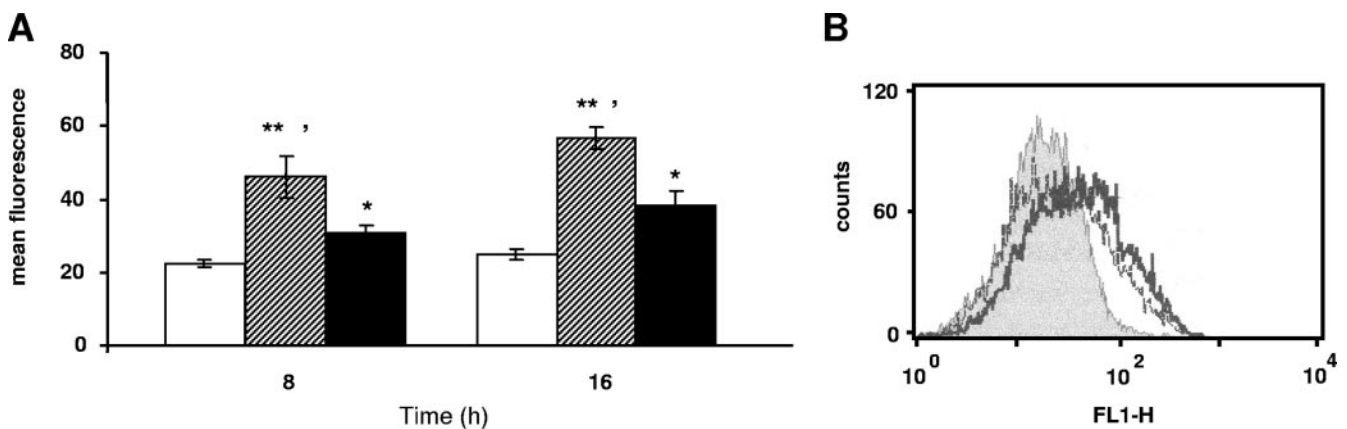

FIG. 1. Expression of ICAM-1 on HBMEC at 8 h and 16 h after incubation with the MC58 (striped bars) and MC58 *siaD* (black bars) strains at an MOI of 10 in comparison to that on uninfected HBMEC (open bars). Results are expressed as means and standard errors of the means for four independent experiments. *, $P < 0.05$ in comparison with uninfected HBMEC; **, $P < 0.01$ in comparison with uninfected HBMEC; ', $P < 0.05$ for ICAM-1 expression on HBMEC after incubation with the MC58 *siaD* strain in comparison to that on cells after incubation with the encapsulated MC58 strain. For comparison, the mean fluorescence intensities for panel A are shown in panel B. FL1-H, fluorescence intensity on channel that detects emissions from fluorescein isothiocyanate.
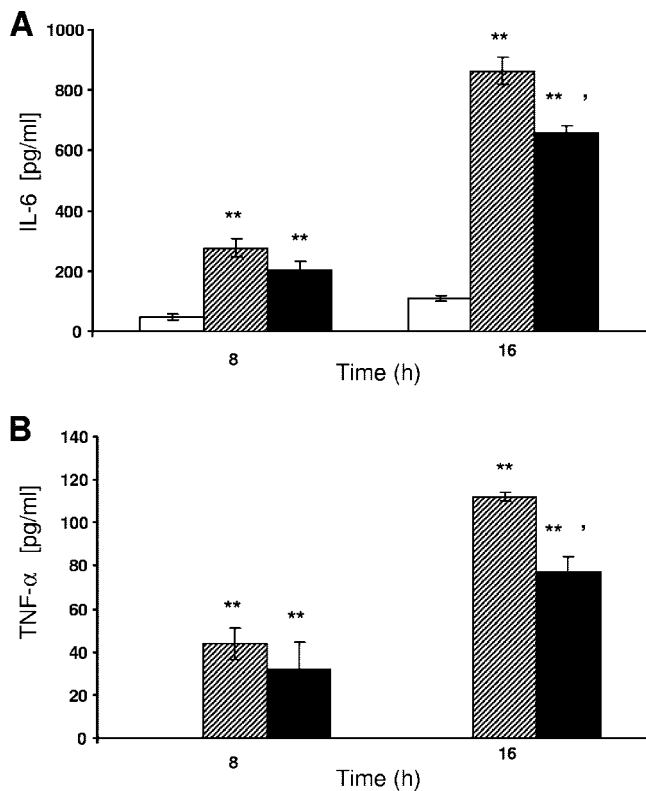
FIG. 2. Concentrations of IL-6 (A) and TNF-α (B) in HBMEC culture supernatant infected with either the MC58 (striped bars) or MC58 *siaD* (black bars) strain for 8 and 16 h. Controls (uninfected cells) are shown as open bars. Cytokine concentrations were assessed by ELISA, and the limits of sensitivity were 4 pg ml^{-1}. Results are expressed as the means ± SEM for four independent experiments carried out in duplicate; **, $P < 0.01$ relative to the respective control; ', $P < 0.01$ compared to the MC58 *siaD* strain.
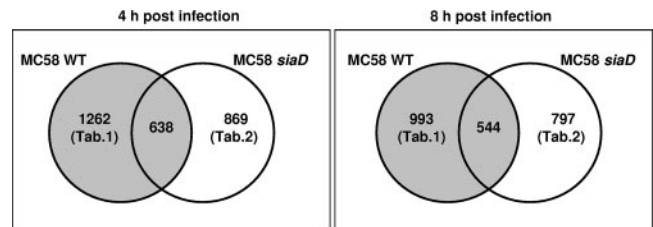

FIG. 3. Schematic representation of the number of regulated HBMEC genes induced following infection with the MC58 and MC58 *siaD* strains at 4 h postinfection (A) and 8 h postinfection (B). Tab., Table.

filament assembly and cell motility, and the Wiskott-Aldrich syndrome protein (WASP).

Capsule-dependent changes in gene expression. Next, we investigated the contribution of the capsular polysaccharide to the observed changes in HBMEC gene expression. For these studies, we took advantage of an unencapsulated mutant of MC58. In this strain, the polysialyltransferase gene *siaD* was inactivated by insertional inactivation as described earlier (60). We adopted a reductionist approach to identify those genes whose expression was influenced by the capsule. First, we used AtlasImage 2.7 software to identify gene expression patterns that were significantly different for MC58 *siaD* mutant-infected cells compared to those for uninfected cells. This comparison revealed 231 genes at 4 h p.i. and 253 genes at 8 h p.i. that were expressed independent of capsule expression (Fig. 3). Analysis with GoMiner revealed an enrichment of genes involved in nucleotide biosynthesis/transcription ($P = 0.02$), metabolism ($P = 0.01$), cell motility ($P = 0.02$), particularly the Arp2/3 protein complex, and regulation of endocytosis ($P = 0.02$). In contrast, expression of 624 genes at 4 h p.i. and 449 genes at 8 h p.i. altered by the encapsulated wild-type strain MC58 were not expressed after infection with the capsule-deficient MC58 *siaD* mutant strain (Fig. 3). This represents 49.4% and 45%, respectively, of the total number of altered genes and suggests that

half of the transcriptional responses of HBMEC are capsule dependent. These genes dependent on capsule expression could be assigned to all functional categories mentioned in Table 1. Table 4 shows the effects of the loss of capsule expression on a selection of genes which participate in the immune response. The capsule-deficient mutant induced more transcript than the WT *N. meningitidis* strain for genes, which are implicated in promoting a proinflammatory response (raw signal intensities higher for the MC58 *siaD* mutant than for the MC58 WT) (see the supplemental material). These patterns were further verified by FACS analysis for ICAM-1 expression (Fig. 1) and ELISA for IL-6 and TNF-α release (Fig. 2).

A total of 638 (at 4 h p.i.) and 544 (at 8 h p.i.) genes were expressed in response to both strains. A description of these genes is presented in Table 3, including apoptosis-related genes and genes encoding cytoskeleton/motility proteins, ILK, urokinase plasminogen activator (uPA), and hypoxia-inducible factor 1-responsive RTP801.

Apoptosis-associated proteins. Numerous HBMEC genes induced after meningococcal infection affected apoptosis. A number of key proapoptotic genes were up-regulated at 4 h p.i., including members of the Bcl2 family (*bak* and *bad*) and genes for calpain (MC58 *siaD* mutant at 4 h p.i. and 8 h p.i.), Fas-activated serine/threonine kinase, and apoptosis-specific protein, while *bax* and the death-associated protein 3 gene were down-regulated (Table 3). At the same time, several antiapoptotic genes were down-regulated, *bclX*, *dad1*, and the adenosine A1 receptor and Akt1 genes, while immediate-early response gene 1 was up-regulated. The regulation of TNF receptor-associated factor 1, which belongs to the "inhibitor of apoptosis" family, was time dependent, being down-regulated at 4 h p.i. and strongly up-regulated at 8 h p.i.

Infection-induced effects on host cell death. Since array data revealed up-regulation of proapoptotic genes and at the same time down-regulation of antiapoptotic genes in HBMEC, we next determined whether incubation with *N. meningitidis* leads to apoptosis in cultured HBMEC. There are conflicting reports in the literature regarding apoptosis induction by *N. meningitidis* (8, 33, 34, 39, 40). We selected different assays that cover a range of apoptotic events in human cells. In order to confirm the array data, real-time PCR was used to quantify gene expression of representative genes in MC58-infected HBMEC. The method described by Pfaffl (46) was used to calculate the changes in target gene expression relative to those in housekeeping gene expression (β-actin) (Table 4) . All genes that showed at least twofold regulated expression, as seen in the

TABLE 3. Effect of capsule deletion on gene expression[a]

Category and array location	Expression in MC58 at 4 h p.i.	Expression in MC58 siaD strain at 4 h p.i.	Expression in MC58 at 8 h p.i.	Expression in MC58 siaD strain at 8 h p.i.	Gene or protein description/name	GenBank accession no.
Cell adhesion receptors						
I02ab6	↑	↑	↑	↑	Intercellular adhesion molecule 1 (CD54), human rhinovirus receptor	NM_000201
Cell signaling/extracellular communication proteins						
F21ef7	*	↑	↑	↑	Interleukin 6 (interferon beta 2)	X04602
I10ef7	*	↑	↑	↑	Tumor necrosis factor, alpha-induced protein 2	M92357
Cell surface antigens						
O21ef1	3.4	*	2.85	3.55	CD44 antigen	M59040
Apoptosis-associated proteins						
A08ef6	0.1	0.2	0.466	0.333	Adenosine A1 receptor	S56143
G14ef6	0.344	*	0.363	0.48	Defender against cell death 1	D15057
G04ef6	3.0	5.0	↑	↑	Immediate-early response 3	AF071596
K24ef1	↑	↑	↑	↑	Bcl2 antagonist of cell death	U66879
N04ab3	*	*	↑	↑	Bcl2 antagonist/killer 1	NM_001188
N23ab2	↑	*	↑	↑	APG5 autophagy 5 like (*S. cerevisiae*)	NM_004849
Cytoskeleton/motility proteins						
C24cd3	2.3	1.2	2.833	2.666	Vimentin	NM_003380
D19ab2	*	*	↑	↑	Actin-related protein 3 homolog (yeast)	NM_005721
Intracellular transducers/ effectors/modulators						
H08ef5	2.0	2.5	1.692	*	Integrin-linked kinase	U40282
Protein turnover						
P19ef7	*	*	↑	↑	Plasminogen activator, urokinase	M15476
Not classified						
C05gh3	3.333	3.0	*	1.09	Hypoxia-inducible factor 1-responsive RTP801	NM_019058

[a] The ratios (numerical values) were calculated as the adjusted intensity of array 2 (MC58- and MC58 siaD strain-infected HBMEC) divided by the adjusted intensity of array 1 (uninfected HBMEC) according to the manufacturer's guidelines. Differences are estimated when a gene signal either in array 1 or in array 2 is at background level. Instead of numerical values, genes are indicated as up-regulated (↑) or down-regulated (↓) in infected HBMEC. * indicates genes with signal intensities of at least twofold over background in infected and uninfected cells.

TABLE 4. Confirmation of expression analysis findings by real-time PCR[a]

Gene	Expression ratio at 4 h p.i.				Expression ratio at 8 h p.i.			
	MC58 WT		MC58 siaD strain		MC58 WT		MC58 siaD strain	
	Array	QRT-PCR	Array	QRT-PCR	Array	QRT-PCR	Array	QRT-PCR
bad	↑	3.23	↑	2.16	↑	4.45	↑	3.33
bak	*	0.10	*	0.22	↑	2.29	↑	2.0
asp	↑	1.14	*	0.87	↑	10.91	↑	26.41
req	*	1.07	*	0.66	↑	4.58	↑	2.63
IEX1	3.0	5.1	5.0	6.55	↑	10.14	↑	11

[a] Confirmation of microarray findings by real-time quantitative reverse transcriptase PCR (QRT-PCR). The ratios (numerical values) were calculated as the adjusted intensity of array 2 (MC58 WT- or MC58 siaD strain-infected HBMEC) divided by the adjusted intensity of array 1 (uninfected HBMEC) according to the manufacturer's guidelines. Differences are estimated when a gene signal either in array 1 or in array 2 is at background level. IEX1, immediate-early response gene 1; ↑, up-regulated. * indicates genes with signal intensities of at least twofold over background in infected and uninfected cells.

arrays compared to the controls, were regulated (except for apoptosis-specific protein up-regulation at 4 h p.i. after MC58 exposition), confirming the up-regulation of those genes already found to be regulated in the array analysis. We next monitored phosphatidylserine translocation on the cell surface by using annexin V staining and FACS analysis. After 8 h of infection, HBMEC exhibited no changes in annexin V staining (Fig. 4A). However, after 24 h of incubation, about 12% of cells were annexin V positive in response to MC58 (Fig. 4B). Infection with the unencapsulated MC58 siaD mutant revealed about 4% annexin V-positive cells.

Infection of HBMEC with *N. meningitidis* leads to caspase 3 and AMPK-α activation and Akt kinase inhibition. Further experiments were carried out to determine whether infection of HBMEC with *N. meningitidis* leads to apoptosis in HBMEC. Assays for caspase 3 and AMPK-α activation were carried out by Western blot analysis. We decided to measure caspase 3 activation as an indicator of apoptosis induction since different upstream pathways leading to apoptosis depend on caspase 3 induction for final apoptotic execution. The kinetics of protein
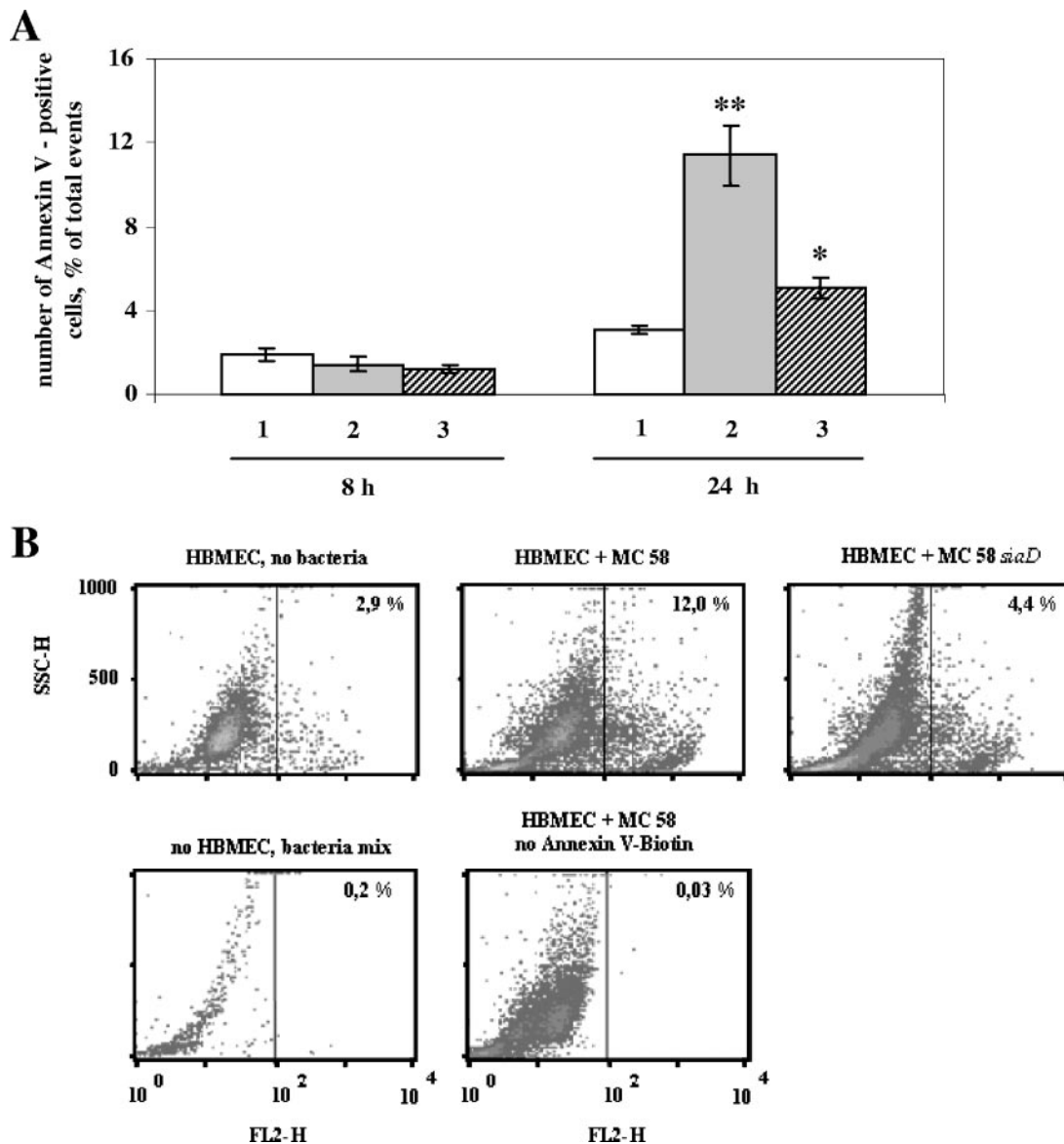
FIG. 4. Annexin V-biotin binding by *N. meningitidis*-infected HBMEC. (A) Percentage of annexin V-biotin-positive cells in HBMEC culture, which was left untreated (1) or which was infected with strain MC58 (2) or the capsule-deficient MC58 *siaD* mutant (3) for 8 and 24 h (MOI, 10). After infection, cells were trypsinized, stained with annexin V-biotin, and detected using streptavidin-phycoerythrin conjugate by flow cytometry. Data represent means ± SEM for four independent experiments. *, $P < 0.05$ compared with the respective control; **, $P < 0.01$ compared with the respective control. (B) Representative dot plots of untreated HBMEC or cells infected with MC58 and the MC58 *siaD* mutant strain for 24 h (MOI, 10). Controls of specificity were used. Bacterial samples were incubated with annexin V-biotin. HBMEC infected with the MC58 WT were measured without primary annexin V-biotin staining. FL2-H, forward scattering intensity; SSC-H, side scattering intensity.

activation was assessed using antibodies that specifically recognized the cleaved caspase 3 (p17 and p19 subunits) and the phosphorylated forms of AMPK-α. Cell lysates prepared from uninfected HBMEC, cultured in the presence of human serum, were used as a control. As shown in Fig. 5, the unencapsulated *N. meningitidis* MC58 *siaD* strain induced cleavage of caspase 3 at 8 h of infection, with an increase of the large 17-kDa cleaved fragment after 24 h of infection. Furthermore, the unencapsulated mutant strain induced more cleaved 17-kDa fragment than the encapsulated parent strain (2.5- and 2.0-fold higher, as estimated by densitometry evaluation) (Fig. 5B).

Since AMPK was demonstrated to be able to participate in apoptosis regulation (4, 28), we next investigated the effects of meningococci on AMPK activity in HBMEC. AMPK has been described to be activated during cellular and environmental stress and regulates energy and metabolic homeostasis of the cell (22, 37). AMPK-α phosphorylation was detected after 24 h of infection in response to the MC58 and MC58 *siaD* strains (Fig. 5A). Wild-type and capsule-deficient MC58 bacteria led to almost identical increases of AMPK-α activity compared to uninfected cells (Fig. 5B). Moreover, expression analyses detected that the mRNAs of protein kinase B or Akt (PKB/Akt) showed a decrease in infected cells (Table 2). The serine-threonine protein kinase Akt is a multifunctional regulator of cell growth and glucose
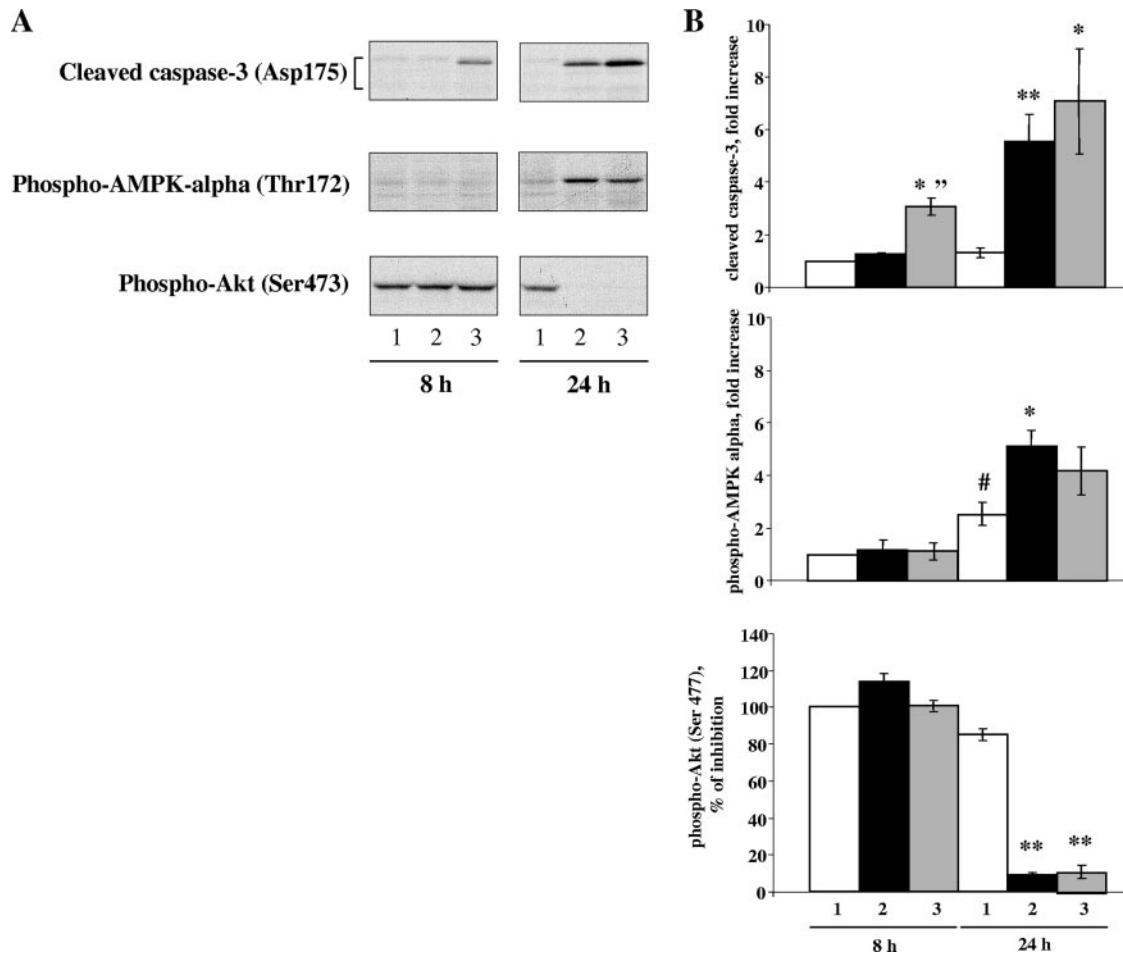
FIG. 5. Effect of *N. meningitidis* infection on caspase 3, AMPK-α, and Akt activities in HBMEC. (A) HBMEC (10^5 ml^{-1}) were incubated with the MC58 and MC58 *siaD* strains (10^6 CFU ml^{-1}) at 37°C for the time indicated. Cellular proteins were separated by SDS-polyacrylamide gel electrophoresis, and Western blotting was performed using antibodies specific for the phosphorylated and nonphosphorylated forms of the proteins of interest, as described in Materials and Methods. The results are representative of four identical experiments with (1) uninfected cells (control), (2) MC58-infected HBMEC, and (3) MC58 *siaD* strain-infected HBMEC. (B) The amounts of cleaved caspase 3, phosphorylated AMPK-α, and Akt were estimated by an NIH image analyzer program, and the mean increases (*n*-fold) or percentages of inhibition ± SEM were calculated. *, $P < 0.05$ relative to the respective control; **, $P < 0.01$ relative to the respective control; #, $P < 0.05$ relative to uninfected cells at 8 h of infection;", $P < 0.01$ compared with controls.

metabolism and is crucial to endothelial cell survival (13, 19). PKB/Akt either directly phosphorylates transcription factors that control the expression of pro- and antiapoptotic genes or promotes survival by directly phosphorylating key regulators of the apoptotic cascade (e.g., Bad) (44). In order to determine whether infection of HBMEC with meningococci not only decreased gene expression but also changed Akt activity, Western blot analyses were performed. After 8 h of infection, there was no visible effect on Akt activity (Fig. 5A). However, after 24 h of infection, we detected a marked inhibition of Akt phosphorylation in HBMEC infected with the MC58 and MC58 *siaD* strains by about 76.0% and 76.2%, respectively.

DISCUSSION

The present study demonstrates the use of cDNA microarray technology to characterize transcriptional responses in HBMEC to infection with the meningitis-causing pathogen *N.*

meningitidis. Brain endothelial cells constitute the B-CSF barrier and are the first line the meningococcus has to overcome to reach the CSF (41, 43). This work represents the first investigation of the global transcriptional response of a key cell affected in the pathogenesis of meningococcal disease. More than 11,000 genes of HBMEC have been analyzed in this study, and distinct changes of host cell gene expression have been observed at 4 and 8 h of infection. This study demonstrates that meningococcal infection induces significant changes of the transcriptome, affecting 7 to 12% of genes (depending on the strain and time point of investigation). Most of the differentially regulated genes are involved in transcription, RNA processing/turnover/transport, translation, and posttranslational modification/protein folding, demonstrating very high activity of nucleic acid turnover in the endothelial cells upon bacterial infection. The genes involved in cell metabolism, particularly in energy production, were found to be one of the groups of genes with increased transcription in infected cells. Our anal-

yses furthermore showed that already at 4 h p.i., about 30% of the regulated genes were up-regulated in infected cells (30% for MC58 and 30.5% for the unencapsulated MC58 *siaD* mutant) and about 70% genes were down-regulated. Interestingly, at 8 h p.i., the expression rates turned around: 77% of the regulated genes in cells infected with MC58 and 66% of genes infected with the MC58 *siaD* strain were up-regulated; 23% and 34% of genes, respectively, were down-regulated in HBMEC infected with wild-type and capsule-deficient bacteria. Although there is no experimental proof at this stage of our analysis, we assume that the majority of differential gene expression is caused by adherent meningococci, because less than 1% of HBMEC were infected with encapsulated meningococci (60; data not shown) and this might not be sufficient for the detection of significant transcriptional changes.

Meningococci have developed different strategies to exploit host cell function for infection, when at the same time the host cell develops an immune response to hinder bacterial infection and multiplication. In general, the host defense against the pathogen includes cytokines, chemokines, and oxidative burst. Among the genes expressed following infection, we found genes involved in the immunological responses, such as those encoding IL-6 and TNF-α, both described to be induced after *N. meningitidis* infection (7, 51, 57, 64). However, absent from the transcriptional profile was IL-1β, which is involved in the pathogenesis of bacterial meningitis. The absence of elevated IL-1β transcripts in infected HBMEC was already observed in meningeal cells (64). Other infection-induced HBMEC genes specifically involved in neutrophil recruitment were the ICAM-1 gene, which, when up-regulated, leads to enhanced adhesion of neutrophils to the brain endothelium (14, 15, 32).

The major virulence factor of *N. meningitidis* is the polysaccharide capsule, which mediates resistance to phagocytosis and promotes bacterial survival in the bloodstream. We analyzed gene expression during infection with an unencapsulated mutant of strain MC58 and found that half of the transcriptional changes (49.4% at 4 h p.i. and 58% at 8 h p.i.) depended on the presence of the capsule. The capsule-dependent genes could be associated with all functional categories mentioned in this study. In the case of certain key immune response genes, gene expression was greater in response to the capsule-deficient mutant than in response to the wild-type strain, suggesting that the meningococcal polysaccharide capsule plays a limiting role in the induction of an inflammatory response. These observations might implicate a mechanism of the bacterium for circumvention of the innate immune system and inhibition of cytokine secretion. Interestingly, the capsule of group B streptococcus, which is also composed of sialic acid, was also assumed to represent a form of molecular mimicry whereby the bacterium resembles host cell surfaces to inhibit immune activation (16).

Successful invasion of meningococci in HBMEC is dependent on endothelial cell cytoskeleton reorganization. Expression analysis revealed that genes coding for cytoskeleton proteins were found to be expressed at high levels, indicating cytoskeletal rearrangements in the context of bacterial internalization. For example, the ARP3 homolog, the actin-related protein 2/3 complex, subunit 2 (p34-Arc), the mRNA of ACTN1, and cytoskeletal gamma actin and alpha 2 actin were highly expressed in infected HBEMC. The Arp2/3 protein complex has been implicated in the control of actin polymer-ization in cells. In mammals, the ARP2/3 complex comprises the two actin-related proteins ARP2 and ARP3 and five additional subunits, p41-Arc, p34-Arc, p21-arc, p20-Arc, and p16-Arc (9). The p34-arc (ARC34) gene, one of the genes which were found to be up-regulated in our study, has been shown to localize to the lamellipodia of stationary and motile fibroblasts as well as to the actin tails assembled by *Listeria monocytogenes*. At the same time, transcript levels of VASP, which is involved in the regulation of the actin filament assembly and cell motility, and WASP, an important VASP cooperator in the stimulation of actin assembly and membrane protrusion, were down-regulated during meningococcal infection. The role of these proteins in regulating actin filaments during *N. meningitidis* infection has not been analyzed yet. However, the findings of the present study are important, taking into account that the existing literature provides no information about WASP/VASP regulation at the transcriptional and translation levels or the role of this protein in meningococcal infection. In a recent study, we demonstrated that meningococci enter HBMEC via fibronectin and binding to $\alpha_5\beta_1$ integrins (60). $\alpha_5\beta_1$ integrins are known to interact with cytoskeletal components, such as talin and α-actinin, in the complex structure associated with focal contacts (26, 31). We therefore searched for the expression of these cytoskeleton proteins and observed up-regulation of ACTN1 and talin 1 (for MC58 at 8 h p.i.). Beneath stimulation of cytoskeleton rearrangements, integrins may activate intracellular cascades of signaling events leading to the modulation of gene expression. In this context, it is notable that mRNA of the ILK was up-regulated in infected HBMEC in response to both meningococcal isolates. ILK was recently described to act as an essential link between integrins and the uptake of group A streptococci into epithelial cells (63). In the present study, it now becomes evident that there is also increased transcriptional activity of negative regulators of the MAPK signaling pathways. For example, members of DUSP1, DUSP5, and DUSP14 and GPS2 were up-regulated during infection. Dual-specificity phosphatases dephosphorylate residues within MAPK and thereby negatively regulate the activity (6). GPS2 was found to potently suppress RAS- and MAPK-mediated signals and interferes with Jun N-terminal protein kinase activity, suggesting that the function of this gene may be repression signaling (54). These findings suggest that increased activation of specific MAPK signaling pathways is negatively controlled by diverse mechanisms, which then might limit the uptake of meningococci in already infected cells.

Expression analysis showed further up-regulation of uPA in infected cells. uPA is a serine protease that converts plasminogen to plasmin, which then acts as a broad-spectrum protease to promote degradation of the extracellular matrix proteins. Meningococci have been shown to be capable of binding plasminogen on its surface, and specific receptors were recently characterized (58). One of the two major plasminogen activators, tissue-type plasminogen activator, has been reported to be specifically bound on the bacterial surface (59). Induction of the second plasminogen activator, uPA, in the infected cell by the bacterium could be an alternative mechanism for plasminogen activation.

Interestingly, mRNA transcript levels of ephrins (Eph) and ephrin receptors (EphA2 and EphA5) were also changed in infected HBMEC. In this context, it is interesting to note that

Plant and coworkers also detected up-regulation of ephrin receptors (EphA2 and EphA3) in ME-180 cells in response to a piliated *N. gonorrhoeae* strain and the *N. meningitidis* strain FAM20 (47). Eph receptors represent the largest class of receptor tyrosine kinases, and together with their ephrin ligands, they are important mediators of cell-cell communication as well as of vascular endothelial cells and specialized epithelia, regulating cell attachment, shape, and motility (23, 29).

Apoptosis is a highly controlled ATP-dependent form of cell death morphologically characterized by chromatin condensation, nuclear fragmentation, cell shrinkage, and blebbing of the plasma membrane (20, 49). The end point of apoptosis is fragmentation of the cell into small membrane-bound bodies that are quickly cleared by phagocytotic cells. Biochemically, apoptosis is characterized by the activation of caspases, highly specific proteases, which cleave a wide range of intracellular substrates. Several studies have reported that endothelial cell injury and/or death is a key pathological finding during bacterial sepsis. As several proapoptotic genes were up-regulated and antiapoptotic genes were mainly down-regulated, we decided to analyze in detail the differential expression of apoptosis-related genes in HBMEC in response to *N. meningitidis* infection. The expression profile of apoptosis-related genes was confirmed by real-time PCR and different assays that cover a range of key apoptotic events in human cells. HBMEC were incubated for different time intervals (up to 24 h) with live intact *N. meningitidis* cells. Cell viability was assessed by the determination of, namely, phosphatidylserine translocation and activation of caspase 3 and AMPK-α. Furthermore, Western blot analysis revealed that *N. meningitidis* infection leads to a marked decrease of PKB/Akt activity, shown by dephosphorylation. The serine-threonine protein kinase Akt has emerged as a crucial regulator of widely divergent cellular processes, including apoptosis, differentiation, and metabolism (44). PKB/Akt promotes cell survival so that it either participates directly in the apoptotic cascade (e.g., phosphorylation of Bad) or regulates the transcription of pro- and antiapoptotic genes. Therefore, our data show that PBK/Akt is not only regulated at the transcriptional level during meningococcal infection but also regulated through dephosphorylation and thus inactivation. Two groups of investigators have analyzed in detail the induction of apoptosis by pathogenic neisseriae in HeLa cells. Müller and coworkers postulated that apoptosis is induced in HeLa cells by either a native or recombinant gonococcal porin, PIB, or intact gonococci (39, 40). Massari and coworkers demonstrated that purified PorB from *N. meningitidis* or PorB from live bacteria associated with mitochondria prevents apoptosis (34). The data presented in this study underline the evidence that *N. meningitidis* induces apoptosis in host cells, although we cannot exclude that the contrasting results might represent different responses as a result of intrinsic differences in various cell types.

One of the key factors in the development of meningococcal shock is increased microvascular permeability (11, 25, 27, 36). Inflammatory changes in microvascular permeability are correlated with the reorganization and widening of interendothelial junctions that are the main structures of B-CSF organization. Lipid mediators, proteases, or cytokines released by infected endothelial cells can affect cytoskeleton organization and endothelium integrity. Expression analysis revealed that genes encoding several structural proteins of endothelial tight and adherent junctions during meningococcal infection were significantly regulated. Transcripts for claudins 12 and 14 and protocadherins 8 and 17 were decreased following infection. Claudins are transmembrane proteins of tight junctions and take part in the regulation of brain endothelial permeability (35). There is accumulating evidence that claudins constitute the backbone of tight-junction strands and that some claudins are expressed in specific cell types: for example, claudin 5 is expressed primarily in endothelial cells of blood vessels (38). Protocadherins constitute the largest subgroup within the cadherin family of calcium-dependent cell-cell adhesion molecules and, because of their presence at cellular junctions, are assumed to be anchored to the cytoskeleton, similar to the classical cadherins (18).

In summary, the present study shows that profiling gene expression patterns in HBMEC and comparing two biological samples of cells provide global information about the interaction between the host cell and the pathogenic bacteria. Furthermore, array studies on host cell responses to infection can be enlarged by analyzing the role of action of specific virulence factors, e.g., capsule polysaccharide. These analyses build up a new platform for further molecular and cellular work to clarify the response profile of endothelial cells to *N. meningitidis* infection and to determine what molecular processes trigger the outcome of meningitis.

REFERENCES

1. **Badger, J. L., C. A. Wass, and K. S. Kim.** 2000. Identification of Escherichia coli K1 genes contributing to human brain microvascular endothelial cell invasion by differential fluorescence induction. Mol. Microbiol. **36:**174–182.
2. **Bhattacharjee, A. K., H. J. Jennings, C. P. Kenny, A. Martin, and I. C. Smith.** 1975. Structural determination of the sialic acid polysaccharide antigens of Neisseria meningitidis serogroups B and C with carbon 13 nuclear magnetic resonance. J. Biol. Chem. **250:**1926–1932.
3. **Binnicker, M. J., R. D. Williams, and M. A. Apicella.** 2003. Infection of human urethral epithelium with Neisseria gonorrhoeae elicits an upregulation of host anti-apoptotic factors and protects cells from staurosporine-induced apoptosis. Cell. Microbiol. **5:**549–560.
4. **Blázquez, C., M. J. Geelen, G. Velasco, and M. Guzman.** 2001. The AMP-activated protein kinase prevents ceramide synthesis de novo and apoptosis in astrocytes. FEBS Lett. **489:**149–153.
5. **Bonnah, R. A., M. U. Muckenthaler, H. Carlson, B. Minana, C. A. Enns, M. W. Hentze, and M. So.** 2004. Expression of epithelial cell iron-related genes upon infection by Neisseria meningitidis. Cell. Microbiol. **6:**473–484.
6. **Camps, M., A. Nichols, and S. Arkinstall.** 2000. Dual specificity phosphatases: a gene family for control of MAP kinase function. FASEB J. **14:**6–16.
7. **Christodoulides, M., B. L. Makepeace, K. A. Partridge, D. Kaur, M. I. Fowler, R. O. Weller, and J. E. Heckels.** 2002. Interaction of *Neisseria meningitidis* with human meningeal cells induces the secretion of a distinct group of chemotactic, proinflammatory, and growth-factor cytokines. Infect. Immun. **70:**4035–4044.
8. **Constantin, D., D. Ala'Aldeent, and S. Murphy.** 2002. Transcriptional activation of nitric oxide synthase-2, and NO-induced cell death, in mouse cerebrovascular endothelium exposed to Neisseria meningitidis. J. Neurochem. **81:**270–276.
9. **Cossart, P.** 2000. Actin-based motility of pathogens: the Arp2/3 complex is a central player. Cell. Microbiol. **2:**195–205.
10. **Cywes, C., I. Stamenkovic, and M. R. Wessels.** 2000. CD44 as a receptor for colonization of the pharynx by group A streptococcus. J. Clin. Investig. **106:**995–1002.

11. **de Kleijn, E. D., J. A. Hazelzet, R. F. Kornelisse, and R. de Groot.** 1998. Pathophysiology of meningococcal sepsis in children. Eur. J. Pediatr. **157:** 869–880.

12. **Dietrich, G., S. Kurz, C. Hubner, C. Aepinus, S. Theiss, M. Guckenberger, U. Panzner, J. Weber, and M. Frosch.** 2003. Transcriptome analysis of *Neisseria meningitidis* during infection. J. Bacteriol. **185:**155–164.

13. **Dimmeler, S., B. Assmus, C. Hermann, J. Haendeler, and A. M. Zeiher.** 1998. Fluid shear stress stimulates phosphorylation of Akt in human endothelial cells: involvement in suppression of apoptosis. Circ. Res. **83:**334–341.

14. **Dixon, G. L. J., R. S. Heyderman, K. Kotovicz, D. L. Jack, S. R. Andersen, U. Vogel, M. Frosch, and N. Klein.** 1999. Endothelial adhesion molecule expression and its inhibition by recombinant bactericidal/permeability-increasing protein are influenced by the capsulation and lipooligosaccharide structure of *Neisseria meningitidis.* Infect. Immun. **67:**5626–5633.

15. **Dixon, G. L., R. S. Heyderman, P. van der Ley, and N. J. Klein.** 2004. High-level endothelial E-selectin (CD62E) cell adhesion molecule expression by a lipopolysaccharide-deficient strain of Neisseria meningitidis despite poor activation of NF-kappaB transcription factor. Clin. Exp. Immunol. **135:**85–93.

16. **Doran, K. S., G. Y. Liu, and V. Nizet.** 2003. Group B streptococcal beta-hemolysin/cytolysin activates neutrophil signaling pathways in brain endothelium and contributes to development of meningitis. J. Clin. Investig. **112:**736–744.

17. **Estabrook, M. M., D. Zhou, and M. A. Apicella.** 1998. Nonopsonic phagocytosis of group C *Neisseria meningitidis* by human neutrophils. Infect. Immun. **66:**1028–1036.

18. **Frank, M., and R. Kemler.** 2002. Protocadherins. Curr. Opin. Cell Biol. **14:**557–562.

19. **Fujio, Y., and K. Walsh.** 1999. Akt mediates cytoprotection of endothelial cells by vascular endothelial growth factor in an anchorage-dependent manner. J. Biol. Chem. **274:**16349–16354.

20. **Granville, D. J., C. M. Carthy, D. W. Hunt, and B. M. McManus.** 1998. Apoptosis: molecular aspects of cell death and disease. Lab. Investig. **78:** 893–913.

21. **Greiffenberg, L., W. Goebel, K. S. Kim, I. Weiglein, A. Bubert, F. Engelbrecht, M. Stins, and M. Kuhn.** 1998. Interaction of *Listeria monocytogenes* with human brain microvascular endothelial cells: InlB-dependent invasion, long-term intracellular growth, and spread from macrophages to endothelial cells. Infect. Immun. **66:**5260–5267.

22. **Hawley, S. A., M. Davison, A. Woods, S. P. Davies, R. K. Beri, D. Carling, and D. G. Hardie.** 1996. Characterization of the AMP-activated protein kinase kinase from rat liver and identification of threonine 172 as the major site at which it phosphorylates AMP-activated protein kinase. J. Biol. Chem. **271:**27879–27887.

23. **Himanen, J. P., and D. B. Nikolov.** 2003. Eph receptors and ephrins. Int. J. Biochem. Cell Biol. **35:**130–134.

24. **Hoffmann, I., E. Eugene, X. Nassif, P. O. Couraud, and S. Bourdoulous.** 2001. Activation of ErbB2 receptor tyrosine kinase supports invasion of endothelial cells by Neisseria meningitidis. J. Cell Biol. **155:**133–143.

25. **Holland, P. C., D. Thompson, S. Hancock, and D. Hodge.** 2002. Calciphylaxis, proteases, and purpura: an alternative hypothesis for the severe shock, rash, and hypocalcemia associated with meningococcal septicemia. Crit. Care Med. **30:**2757–2761.

26. **Horwitz, A., K. Duggan, C. Buck, M. C. Beckerle, and K. Burridge.** 1986. Interaction of plasma membrane fibronectin receptor with talin—a transmembrane linkage. Nature **320:**531–533.

27. **Klein, N. J., C. A. Ison, M. Peakman, M. Levin, S. Hammerschmidt, M. Frosch, and R. S. Heyderman.** 1996. The influence of capsulation and lipooligosaccharide structure on neutrophil adhesion molecule expression and endothelial injury by Neisseria meningitidis. J. Infect. Dis. **173:**172–179.

28. **Kobayashi, H., N. Ouchi, S. Kihara, K. Walsh, M. Kumada, Y. Abe, T. Funahashi, and Y. Matsuzawa.** 2004. Selective suppression of endothelial cell apoptosis by the high molecular weight form of adiponectin. Circ. Res. **94:**e27–31.

29. **Kullander, K., and R. Klein.** 2002. Mechanisms and functions of Eph and ephrin signalling. Nat. Rev. Mol. Cell Biol. **3:**475–486.

30. **Lu, S. J., F. Li, L. Vida, and G. R. Honig.** 2004. CD34+CD38− hematopoietic precursors derived from human embryonic stem cells exhibit an embryonic gene expression pattern. Blood **103:**4134–4141.

31. **Luna, E. J., and A. L. Hitt.** 1992. Cytoskeleton—plasma membrane interactions. Science **258:**955–964.

32. **Male, D., J. Rahman, G. Pryce, T. Tamatani, and M. Miyasaka.** 1994. Lymphocyte migration into the CNS modelled in vitro: roles of LFA-1, ICAM-1 and VLA-4. Immunology **81:**366–372.

33. **Massari, P., Y. Ho, and L. M. Wetzler.** 2000. Neisseria meningitidis porin PorB interacts with mitochondria and protects cells from apoptosis. Proc. Natl. Acad. Sci. USA **97:**9070–9075.

34. **Massari, P., C. A. King, A. Y. Ho, and L. M. Wetzler.** 2003. Neisserial PorB is translocated to the mitochondria of HeLa cells infected with Neisseria meningitidis and protects cells from apoptosis. Cell. Microbiol. **5:**99–109.

35. **Matter, K., and M. S. Balda.** 2003. Holey barrier: claudins and the regulation of brain endothelial permeability. J. Cell Biol. **161:**459–460.

36. **Mercier, J. C., F. Beaufils, J. F. Hartmann, and D. Azema.** 1988. Hemodynamic patterns of meningococcal shock in children. Crit. Care Med. **16:**27–33.

37. **Moore, F., J. Weekes, and D. G. Hardie.** 1991. Evidence that AMP triggers phosphorylation as well as direct allosteric activation of rat liver AMP-activated protein kinase. A sensitive mechanism to protect the cell against ATP depletion. Eur. J. Biochem. **199:**691–697.

38. **Morita, K., H. Sasaki, M. Furuse, and S. Tsukita.** 1999. Endothelial claudin: claudin-5/TMVCF constitutes tight junction strands in endothelial cells. J. Cell Biol. **147:**185–194.

39. **Müller, A., D. Gunther, V. Brinkmann, R. Hurwitz, T. F. Meyer, and T. Rudel.** 2000. Targeting of the pro-apoptotic VDAC-like porin (PorB) of Neisseria gonorrhoeae to mitochondria of infected cells. EMBO J. **19:**5332–5343.

40. **Müller, A., D. Gunther, F. Dux, M. Naumann, T. F. Meyer, and T. Rudel.** 1999. Neisserial porin (PorB) causes rapid calcium influx in target cells and induces apoptosis by the activation of cysteine proteases. EMBO J. **18:**339–352.

41. **Nassif, X.** 1999. Interaction mechanisms of encapsulated meningococci with eucaryotic cells: what does this tell us about the crossing of the blood-brain barrier by Neisseria meningitidis? Curr. Opin. Microbiol. **2:**71–77.

42. **Nassif, X., J. L. Beretti, J. Lowy, P. Stenberg, P. O'Gaora, J. Pfeifer, S. Normark, and M. So.** 1994. Roles of pilin and PilC in adhesion of Neisseria meningitidis to human epithelial and endothelial cells. Proc. Natl. Acad. Sci. USA **91:**3769–3773.

43. **Nassif, X., S. Bourdoulous, E. Eugene, and P. O. Couraud.** 2002. How do extracellular pathogens cross the blood-brain barrier? Trends Microbiol. **10:**227–232.

44. **Nicholson, K. M., and N. G. Anderson.** 2002. The protein kinase B/Akt signalling pathway in human malignancy. Cell. Signal. **14:**381–395.

45. **Nizet, V., K. S. Kim, M. Stins, M. Jonas, E. Y. Chi, D. Nguyen, and C. E. Rubens.** 1997. Invasion of brain microvascular endothelial cells by group B streptococci. Infect. Immun. **65:**5074–5081.

46. **Pfaffl, M. W.** 2001. A new mathematical model for relative quantification in real-time RT-PCR. Nucleic Acids Res. **29:**e45.

47. **Plant, L., V. Asp, L. Lovkvist, J. Sundqvist, and A. B. Jonsson.** 2004. Epithelial cell responses induced upon adherence of pathogenic Neisseria. Cell. Microbiol. **6:**663–670.

48. **Prasadarao, N. V., C. A. Wass, S. H. Huang, and K. S. Kim.** 1999. Identification and characterization of a novel Ibe10 binding protein that contributes to *Escherichia coli* invasion of brain microvascular endothelial cells. Infect. Immun. **67:**1131–1138.

49. **Reed, J. C.** 2000. Mechanisms of apoptosis. Am. J. Pathol. **157:**1415–1430.

50. **Rintoul, R. C., R. C. Buttery, A. C. Mackinnon, W. S. Wong, D. Mosher, C. Haslett, and T. Sethi.** 2002. Cross-linking CD98 promotes integrin-like signaling and anchorage-independent growth. Mol. Biol. Cell **13:**2841–2852.

51. **Robinson, K., M. Taraktsoglou, K. S. Rowe, K. G. Wooldridge, and D. A. Ala'Aldeen.** 2004. Secreted proteins from Neisseria meningitidis mediate differential human gene expression and immune activation. Cell. Microbiol. **6:**927–938.

52. **Seger, R., and E. G. Krebs.** 1995. The MAPK signaling cascade. FASEB J. **9:**726–735.

53. **Sokolova, O., N. Heppel, R. Jagerhuber, K. S. Kim, M. Frosch, M. Eigenthaler, and A. Schubert-Unkmeir.** 2004. Interaction of Neisseria meningitidis with human brain microvascular endothelial cells: role of MAP- and tyrosine kinases in invasion and inflammatory cytokine release. Cell. Microbiol. **6:**1153–1166.

54. **Spain, B. H., K. S. Bowdish, A. R. Pacal, S. F. Staub, D. Koo, C.-Y. R. Chang, W. Xie, and J. Colicelli.** 1996. Two human cDNAs, including a homolog of *Arabidopsis FUS6* (*COP11*), suppress G-protein- and mitogen-activated protein kinase-mediated signal transduction in yeast and mammalian cells. Mol. Cell. Biol. **16:**6698–6706.

55. **Stins, M. F., J. Badger, and K. S. Kim.** 2001. Bacterial invasion and transcytosis in transfected human brain microvascular endothelial cells. Microb. Pathog. **30:**19–28.

56. **Stins, M. F., F. Gilles, and K. S. Kim.** 1997. Selective expression of adhesion molecules on human brain microvascular endothelial cells. J. Neuroimmunol. **76:**81–90.

57. **Taha, M. K.** 2000. Neisseria meningitidis induces the expression of the TNF-alpha gene in endothelial cells. Cytokine **12:**21–25.

58. **Ullberg, M., P. Kuusela, B. E. Kristiansen, and G. Kronvall.** 1992. Binding of plasminogen to Neisseria meningitidis and Neisseria gonorrhoeae and formation of surface-associated plasmin. J. Infect. Dis. **166:**1329–1334.

59. **Ullberg, M., B. Wiman, and G. Kronvall.** 1994. Binding of tissue-type plasminogen activator (t-PA) to Neisseria meningitidis and Haemophilus influenzae. FEMS Immunol. Med. Microbiol. **9:**171–177.

60. **Unkmeir, A., K. Latsch, G. Dietrich, E. Wintermeyer, B. Schinke, S. Schwender, K. S. Kim, M. Eigenthaler, and M. Frosch.** 2002. Fibronectin mediates Opc-

dependent internalization of Neisseria meningitidis in human brain microvascular endothelial cells. Mol. Microbiol. **46:**933–946.

61. **Virji, M., H. Kayhty, D. J. Ferguson, C. Alexandrescu, J. E. Heckels, and E. R. Moxon.** 1991. The role of pili in the interactions of pathogenic Neisseria with cultured human endothelial cells. Mol. Microbiol. **5:**1831–1841.

62. **Virji, M., S. M. Watt, S. Barker, K. Makepeace, and R. Doyonnas.** 1996. The N-domain of the human CD66a adhesion molecule is a target for Opa proteins of Neisseria meningitidis and Neisseria gonorrhoeae. Mol. Microbiol. **22:**929–939.

63. **Wang, B., R. S. Yurecko, S. Dedhar, and P. P. Cleary.** 2006. Integrin-linked kinase is an essential link between integrins and uptake of bacterial pathogens by epithelial cells. Cell. Microbiol. **8:**257–266.

64. **Wells, D. B., P. J. Tighe, K. G. Wooldridge, K. Robinson, and D. A. A. Ala' Aldeen.** 2001. Differential gene expression during meningeal-meningococcal interaction: evidence for self-defense and early release of cytokines and chemokines. Infect. Immun. **69:**2718–2722.

65. **Zeeberg, B. R., W. Feng, G. Wang, M. D. Wang, A. T. Fojo, M. Sunshine, S. Narasimhan, D. W. Kane, W. C. Reinhold, S. Lababidi, K. J. Bussey, J. Riss, J. C. Barrett, and J. N. Weinstein.** 2003. GoMiner: a resource for biological interpretation of genomic and proteomic data. Genome Biol. **4:**R28.

Editor: J. N. Weiser